



รายงานการวิจัย

ชุดโครงการวิจัย

การศึกษาวิธีการกำจัดสัญญาณพื้นหลังของเทคนิคการวัดรูปทรงสามมิติ

ดิจิตอลฟูริเยร์ทรานสฟอร์ม

(Investigation of background elimination techniques for digital
Fourier transform profilometry)



ได้รับทุนอุดหนุนการวิจัยจาก
มหาวิทยาลัยเทคโนโลยีสุรนารี



รายงานการวิจัย

ชุดโครงการวิจัย

การศึกษาวิธีการกำจัดสัญญาณพื้นหลังของเทคนิคการวัดรูปทรงสามมิติ

ดิจิตอลฟูรีเยร์ทรานสฟอร์ม

(Investigation of background elimination techniques for digital
Fourier transform profilometry)

หัวหน้าชุดโครงการ

ผู้ช่วยศาสตราจารย์ ดร. พนมศักดิ์ มีมนต์

สาขาวิชาฟิสิกส์

สำนักวิชาวิทยาศาสตร์

โครงการวิจัยย่อย

1. การวิเคราะห์รูปทรงสามมิติแบบดิจิตอลฟูรีเยร์ทรานสฟอร์มโดยการลบสัญญาณตรง (SUT1-107-56-12-38) หัวหน้าโครงการวิจัยย่อย: ผศ.ดร. พนมศักดิ์ มีมนต์
2. การวิเคราะห์รูปทรงสามมิติแบบดิจิตอลฟูรีเยร์ทรานสฟอร์มโดยตัวกรองเวฟเล็ต (SUT1-107-55-12-44) หัวหน้าโครงการวิจัยย่อย: Prof. Dr. Joewono Widjaja

ได้รับทุนอุดหนุนการวิจัยจากมหาวิทยาลัยเทคโนโลยีสุรนารี ปีงบประมาณ พ.ศ. 2556

ผลงานวิจัยเป็นความรับผิดชอบของหัวหน้าโครงการวิจัยแต่เพียงผู้เดียว

กิตติกรรมประกาศ

การวิจัยครั้งนี้ได้รับทุนอุดหนุนการวิจัยจาก มหาวิทยาลัยเทคโนโลยีสุรนารี ประจำปี
งบประมาณ พ.ศ. 2556



บทคัดย่อภาษาไทย

วิทยาการและเทคโนโลยีทางเลเซอร์และโฟตอนิกส์เป็นไปอย่างรวดเร็วและมีการประยุกต์ใช้ในงานด้านต่างๆ อย่างแพร่หลาย ซึ่งระบบเชิงแสงมีความโดดเด่นทั้งในด้านความเร็วและความแม่นยำในการทำงาน จึงเป็นที่นิยมใช้ในงานทางอุตสาหกรรม ทางการแพทย์ รวมถึงทางการทหารและความมั่นคง รวมถึงในชีวิตประจำวันต่างๆ ไปด้วย โดยเฉพาะในทางอุตสาหกรรมและทางการทหารนั้น บ่อยครั้งที่การตรวจวัดลักษณะรูปร่างของวัตถุในเชิงสามมิติแบบละเอียดและไม่สัมผัสซึ่งงานมีความจำเป็นอย่างสูง ในโครงการนี้ ทีมวิจัยมุ่งพัฒนาเทคนิคและระบบต้นแบบในระดับห้องทดลองของระบบที่เรียกว่า Fourier Transform Profilometry (FTP) ซึ่งอาศัยหลักการทางโฮโลกราฟีเพื่อตรวจวัดรูปร่างของวัตถุได้ในระยะไกลโดยการวิเคราะห์เฟสที่เปลี่ยนไปของสัญญาณโฮโลแกรมที่วัดได้

ในชุดโครงการวิจัยนี้ ทีมวิจัยได้พัฒนาเทคนิคใหม่ของการกำจัดสัญญาณพื้นหลังของภาพเกรตติ้ง ซึ่งประกอบไปด้วย 2 เทคนิค ได้แก่ เทคนิคการลบสัญญาณตรง และเทคนิคการแปลงแบบเวฟเล็ต ซึ่งทั้งสองวิธีมีจุดเด่นที่เหมือนกันคือ จะใช้การถ่ายภาพเพียงแค่ครั้งเดียว ระบบการทดลองในระดับห้องปฏิบัติการได้ถูกสร้างขึ้นเพื่อทดสอบประสิทธิภาพและความถูกต้องของเทคนิคที่พัฒนาขึ้น ทั้งนี้ เทคนิคที่น่าเสนาหามีข้อดีกว่าวิธีการเดิมคือ มีต้นทุนการผลิตที่ถูกลง มีขั้นตอนการวัด และการสอบเทียบที่ไม่ซับซ้อน และมีความเร็วของการวัดที่สูง จึงสามารถลดสัญญาณรบกวนจากการสั่นของระบบได้ดี เหมาะกับการนำไปประยุกต์ใช้ในระดับภาคสนามต่อไป

ทั้งนี้ระบบและวิธีการต้นแบบที่พัฒนาขึ้นคาดว่าจะสามารถนำไปประยุกต์กับงานตรวจจับรูปร่าง ความผิดปกติของชิ้นส่วนหรือผลิตภัณฑ์ในอุตสาหกรรมการผลิต รวมไปถึงการประยุกต์ใช้ระบบต้นแบบและองค์ความรู้ที่ได้ในการใช้งานจริงในด้านการวัดรูปร่างสามมิติแบบละเอียดในงานวิจัยอื่นๆ ที่เกี่ยวข้อง เช่น อุตสาหกรรมอิเล็กทรอนิกส์ การตรวจสอบคุณภาพของชิ้นงานแบบอัตโนมัติ ทางการแพทย์และสาธารณสุข และการศึกษาวัตถุโบราณแบบไม่ทำลายล้าง รวมถึงการประยุกต์ใช้ทางการทหารและความมั่นคง เป็นต้น อีกทั้งทีมวิจัยและนักศึกษาผู้มีส่วนร่วมในแผนงานวิจัยได้มีการพัฒนาองค์ความรู้และทักษะในการออกแบบและสร้างระบบเชิงแสงในระดับห้องปฏิบัติการ ซึ่งสอดคล้องกับยุทธศาสตร์การสร้างศักยภาพและความสามารถเพื่อการพัฒนาทางวิทยาการและทรัพยากรบุคคลของประเทศ

บทคัดย่อภาษาอังกฤษ

Fourier transform profilometry (FTP) is one of the useful three-dimensional (3-D) non-contact non-destructive shape measurement methods. When a sinusoidal grating is projected onto an object surface being studied, phase of the projected grating pattern is modulated by spatial profile of the object. This phase modulation is encoded into fundamental frequency spectra of the grating pattern. By recording the deformed grating pattern with an image acquisition sensor, this phase information can be retrieved from the fundamental spectrum by using Fourier transformations. The retrieved phase information is then employed for reconstructing 3-D object surface profile. However besides fundamental components, deformed grating images may also contain lower and higher orders of spectra. When the fundamental component has broad bandwidth, it may be corrupted by the other spectra. This is the inherent drawback of the conventional FTP.

In this project, two new techniques of white light non-phase-shifting for eliminating unwanted background in FTP have been investigated. In the first technique, by using an object image being measured and a single grating image deformed by this object, the background signal of the deformed grating image can be eliminated by using the object image scaled by a contrast ratio of the two images. In the second technique, the background noise is eliminated by utilizing the wavelet transformation.

Both two proposed methods have advantages over the previous works in that firstly, uses of a white light illumination and a monochrome image sensor results in low-cost system. Moreover, the calibration process of the mean and the contrast values is simpler and independent upon characteristics of the image sensors. In addition, the use of a single grating pattern minimizes simultaneously projection and image acquisition times and phase error caused by abrupt change in amplitude or timing of light projector's synchronization signals known as jitters.

Table of Content

กิตติกรรมประกาศ	ก
บทคัดย่อภาษาไทย	ข
บทคัดย่อภาษาอังกฤษ	ค
Table of Content.....	ง
List of Figures	จ
Chapter 1. Introduction.....	1
1.1 Background and Significance	1
1.2 Objectives	2
1.3 Scope.....	2
1.4 Expected Benefit	3
1.5 Research Structure.....	3
Chapter 2. Theory	4
2.1 3D Height Reconstruction Using DC Subtraction	4
2.2 3D Height Reconstruction Using Wavelet Filter	6
Chapter 3. Materials and Methods	8
Chapter 4. Results and Discussions	9
4.1 Experimental Setup of the Frings Projection.....	9
4.2 3D Height Reconstruction Using DC Subtraction	10
4.3 3D Height Reconstruction Using the Wavelet transformation	12
Chapter 5. Conclusions	14
Research Outcome	15
References	16
ประวัตินักวิจัย.....	18

List of Figures

Figure 2.1 A schematic diagram of an optical setup for implementing the proposed	4
Figure 2.2 (a) First and (b) second derivatives of the Gaussian wavelets, respectively.	7
Figure 3.1 An isosceles triangular object.....	8
Figure 4.1 Images of (a) the prism object and (b) the reference plane generated by using uniform light. (c) Grating patterns deformed by (a) the object and (d) Grating patterns on the reference plane in (b).	9
Figure 4.2 Intensities scanned at the row 100th of the grating images deformed by (a) the object and (b) the reference plane. The resultant signals obtained by eliminating the background from (c) Fig. 4.2 (a) and (d) Fig. 4.2 (b).	10
Figure 4.3 Power spectra of the grating pattern deformed by the object obtained by using (a) the conventional FTP and (b) the proposed method.	11
Figure 4.4 Comparison between the height profiles reconstructed by using the conventional FTP, the direct contact and the proposed method.....	11
Figure 4.5 Height reconstructions of the prism generated by using the conventional FTP and the first derivative Gaussian wavelet.	12
Figure 4.6 Height reconstructions of the prism generated by using the conventional FTP and the second derivative Gaussian wavelet.	13

Chapter 1. Introduction

1.1 Background and Significance

Optical methods for three-dimension (3D) shape measurement and imaging have found growing interest in many industrial applications such as object modeling, medical diagnostics, computer-aided design and computer-aided manufacturing. Non contact and non invasive abilities to make such measurements are the reason for this growing interest. Among those methods, Fourier transform profilometry (FTP) has been widely studied [1-6]. The FTP has found various applications in diverse fields such as biomedical applications [7-11], quality control of printed circuit board manufacturing [12-16], kinematic study of a moving creature [17-19], cultural heritage and preservation [20,21], global measurement of free surface deformations [22,23], and biometric identification [24] etc.

One of the outstanding features of the FTP is that the 3D shape measurement can be performed by using only single frame of the fringe pattern deformed by the specimen. Consequently, it is suitable for dealing with dynamic situation where taking more than single frame becomes prohibitive.

In the FTP, a Ronchi grating or a sinusoidal grating pattern is projected onto the specimen to be profiled. To a CCD sensor camera viewing the specimen, height variations of the surface are encoded as phase modulations of the observed fringe pattern, with a sensitivity that depends on the angle between the illumination and observation directions. Accurate and reliable extraction of the phase information is therefore the key to this shape measurement technique. In order to extract the phase variation, a FFT algorithm is used to digitally compute the 1D signal of the deformed grating captured by the CCD. After selecting only the fundamental spatial-frequency spectrum component and taking its inverse Fourier transform, the height information can be decoded from the extracted phase [1,2].

The FTP has a drawback in that deep phase modulation will cause overlapping between the desired fundamental spatial-frequency spectrum and the zero-order spectrum. As a result, the measurable height is limited by the phase modulation. Several methods for solving this drawback by using π -phase shift [25,26], orthogonal gratings [27], and windowed Fourier transform [28] have been reported. The first three methods employ more than one grating pattern. Although subtraction between the deformed patterns generated by the π -phase shift or the orthogonal gratings can eliminate unwanted background. However, they cannot be applied to dynamic measurements. In the later method, a set of Gaussian

windows is used to estimate the zero-order spectrum. The estimated spectrum is then subtracted from the whole spectrum of the deformed grating pattern.

In this project, a new method for eliminating the zero-order spectrum of the FTP by using simple dc subtraction is studied. In the dc subtraction method, the mean value of the deformed grating is calculated and then subtracted from the deformed grating prior to the Fourier transformation process. Since our proposed method employs only single deformed grating pattern, the improved FTP can be used for dynamic 3D shape measurement. Measurement performance of the proposed methods will be compared with that of the phase shift-based FTP.

1.2 Objectives

- 1) To develop a laboratory prototype of the fringe projection FTP
- 2) To verify feasibility of 3D height reconstruction by using the DC subtraction method
- 3) To verify feasibility of 3D height reconstruction by using the Wavelet transformation method
- 4) To develop software for extracting phase modulation and reconstructing 3D height
- 5) To compare the two proposed methods with the conventional methods

1.3 Scope

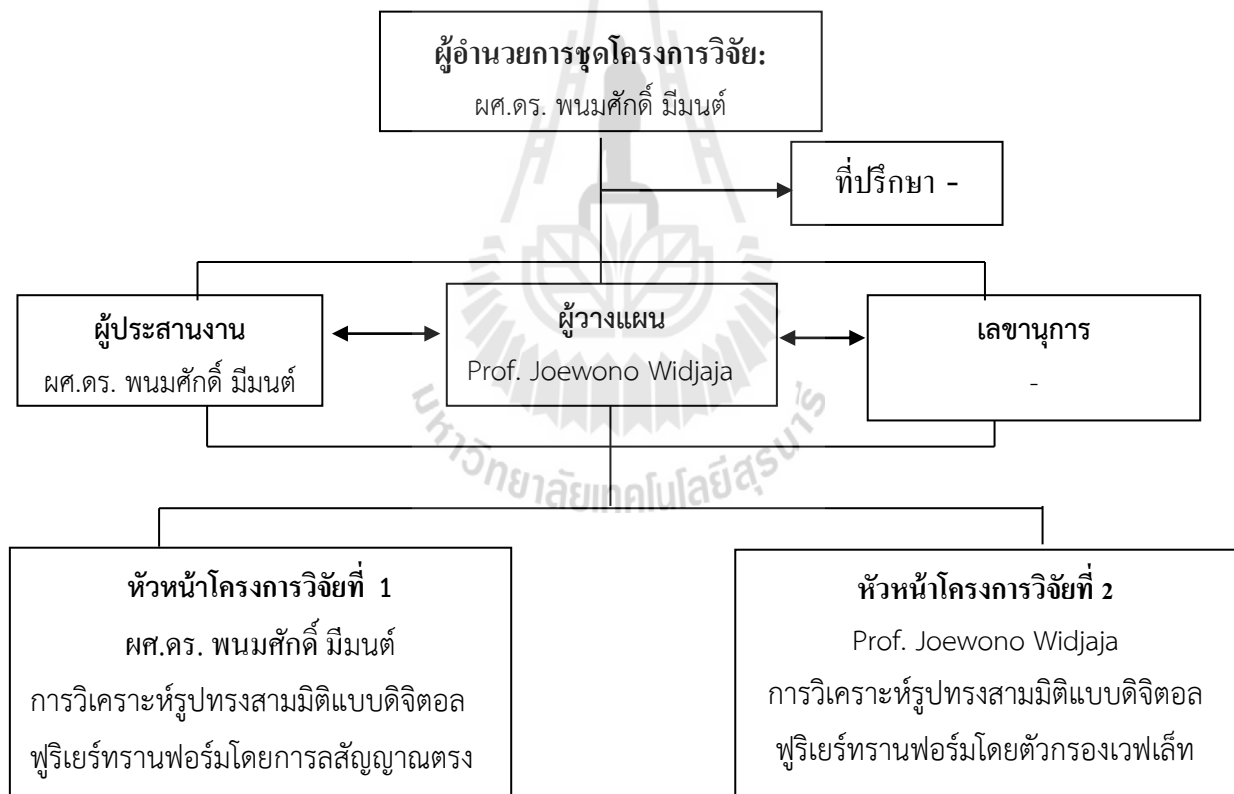
In this study, a sinusoidal grating digitally generated by using a LCD projector is projected onto a 3D test object. The grating patterns deformed by the object and the reference plane are captured by a CCD camera connected to a computer system. We have investigated two technique of background elimination to improve the performance of the 3D reconstruction of the fringe projection FTP. In the first method, the images of the object and the reference plane are recorded. After calculating contrast and filtering out first-order spectrum of each image, the background signal is subtracted from the deformed grating. In the second method, the two grating images deformed by the object and the reference plane are wavelet transformed at an appropriate dilation factor. This step removes the background information. In both methods, the desired phase modulation is then extracted from the background-eliminated deformed gratings. After unwrapping the phase, the height distribution is reconstructed. The determination of the phase modulation and the 3D

reconstruction is done by using Matlab 6.0. Calibration of the system will be done by utilizing a 3D triangular prism with known dimension.

1.4 Expected Benefit

- 1) The result of this research project is useful for electronic manufacturers, automation industries, health care and medical diagnostics, cultural heritage and preservation, security etc.
- 2) Participation of graduate students as research assistant provides an opportunity for developing manpower with capability to conduct research in the area of science, medicine and engineering.

1.5 Research Structure



Chapter 2. Theory

2.1 3D Height Reconstruction Using DC Subtraction

Figure 1 shows a schematic diagram of crossed-optical-axes setup for implementing the proposed method. Under uniform light illumination generated from a LCD projector, the images of the object and the reference plane recorded by a CCD camera can be mathematically expressed as $g_1(x,y) = o(x,y)$ and $g_2(x,y) = r(x,y)$, respectively. Here, $o(x,y)$ and $r(x,y)$ correspond to the irradiances caused by non-uniform light reflection of the object and reference plane. In the case of the illumination by using the sinusoidal grating pattern, the grating images deformed by the object and the reference plane are given by

$$g_3(x, y) = o(x, y) + bo(x, y) \cos[2\pi f_0 x + \phi(x, y)] \quad (1)$$

and

$$g_4(x, y) = r(x, y) + br(x, y) \cos[2\pi f_0 x + \phi_0(x, y)], \quad (2)$$

respectively. In the above equations, f_0 stands for the carrier frequency of the observed grating image, while b is the modulation factor. $\phi(x,y)$ and $\phi_0(x,y)$ are the phase modulations arising from the height profile of the object and the reference plane, respectively. Note that the higher the profile, the broader the phase modulation.

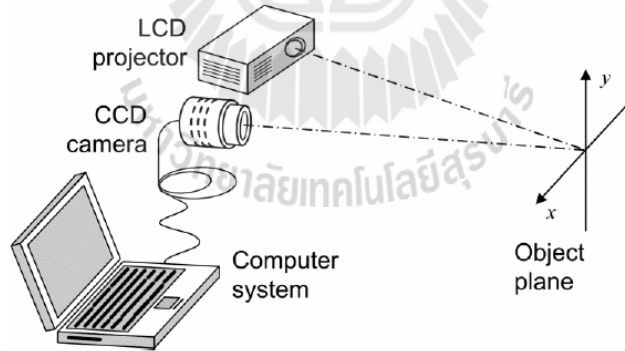


Figure 2.1 A schematic diagram of an optical setup for implementing the proposed FTP by using the dc background subtraction method.

To remove the dc bias from each digital image, its value is determined by

$$g_{dc}(x, y) = \frac{1}{N \times M} \sum_{k=1}^M \sum_{l=1}^N g(k\Delta x, l\Delta y) \quad (3)$$

with N and M are the number of pixels, while Δx and Δy are their corresponding pixel sizes in the horizontal and the vertical directions, respectively. The unwanted backgrounds are then eliminated by the following subtractions

$$\begin{aligned} g'(x, y) &= g_3(x, y) - g_{3dc}(x, y) - [g_1(x, y) - g_{1dc}(x, y)]/c_r' \\ &= bo(x, y) \cos[2\pi f_0 x + \phi(x, y)]/c_r' \end{aligned} \quad (4)$$

and

$$\begin{aligned} g''(x, y) &= g_4(x, y) - g_{4dc}(x, y) - [g_2(x, y) - g_{2dc}(x, y)]/c_r'' \\ &= br(x, y) \cos[2\pi f_0 x + \phi_0(x, y)]/c_r'', \end{aligned} \quad (5)$$

where c_r is the contrast ratio of images obtained with the grating and the uniform light illuminations. The contrast of each image is calculated by using [7]

$$c = \int |G(f_x)| df_x / |G(0)|, \quad (6)$$

where $G(f_x, f_y)$ and $G(0,0)$ correspond to the amplitude spectrum of any image $g(x,y)$ and its zero frequency component. The division of the second terms in Eqs. (4) and (5) by c_r are used to equalize the ac component of the images generated by the grating and the uniform illuminations. This ensures that the unwanted backgrounds are completely eliminated and the desired phase information encoded into the fundamental spectra can be extracted by using the Fourier transformation. By filtering only a single fundamental spectrum and taking its inverse Fourier transform, Eqs. (4) and (5) reduce to

$$g'(x, y) = 0.5bo(x, y) \exp[i\phi(x, y)]/c_r' \quad (7)$$

and

$$g''(x, y) = 0.5br(x, y) \exp[i\phi_0(x, y)]/c_r'', \quad (8)$$

respectively. The phase can be extracted from by taking a complex logarithm of the product of Eq. (7) and the conjugate of Eq. (8)

$$\begin{aligned} \log\{g'(x, y)g''^*(x, y)\} &= \log[0.25b^2 o(x, y)r(x, y)/c_r' c_r''] \\ &\quad + i[\phi(x, y) - \phi_0(x, y)]. \end{aligned} \quad (9)$$

Finally, the height distribution is calculated according to

$$h(x, y) = \frac{l_0[\phi(x, y) - \phi_0(x, y)]}{[\phi(x, y) - \phi_0(x, y)] - 2\pi f_0 d}, \quad (10)$$

where l_0 and d are the separation distances between the CCD camera and the reference plane and between the camera and the projector.

2.2 3D Height Reconstruction Using Wavelet Filter

The definition of the WT of a spatial signal $g(x)$ is given by [21]

$$W_g(a,b) = \frac{1}{\sqrt{a}} \int_{-\infty}^{+\infty} g(x) h^* \left(\frac{x-b}{a} \right) dx, \quad (11)$$

where a and b are the dilation and the translation parameters, respectively. This equation can be interpreted as a cross correlation between the signal $g(x)$ and a set of elementary functions derived by dilating the mother wavelet $h(x)$ which has a response of band-pass filter. In the spatial frequency domain, Eq. (11) can be written as

$$W_g(a,b) = \int_{-\infty}^{+\infty} G(f_x) H_a^*(f_x) \exp(i2\pi x f_x) df_x, \quad (12)$$

which calculated by taking an inverse Fourier transform of a product of two spectra of the signal $g(x)$ and the wavelet $h(x)$ dilated by the factor a .

There are two Gaussian wavelets that are widely used for signal and image analysis. The first wavelet is the first derivative of the Gaussian mother wavelet given by

$$h(x) = \frac{-x}{\sigma^3 \sqrt{2\pi}} \exp\left(-\frac{x^2}{2\sigma^2}\right). \quad (13)$$

The second one is the second derivative of the Gaussian function or the so-called Mexican hat wavelet defined as [32,33]

$$h(x) = \frac{1}{\sigma^3 \sqrt{2\pi}} \left(\frac{x^2}{\sigma^2} - 1 \right) \exp\left(-\frac{x^2}{2\sigma^2}\right). \quad (14)$$

They are illustrated in Figs. 2.2(a) and (b), respectively. Although they are different in the space domain, their frequency responses shown in Figs. 2.3 (a) and (b) have the same characteristics that the frequency response $H(f_x) = 0$ at $f_x = 0$. This is called the admissible condition []. Since this property can simultaneously eliminate the zero order spectrum and localize particular frequency components of signals being analyzed, it is useful for eliminating the background signal. However, a comparison of the two figures reveals that the frequency response of the first-derivative Gaussian wavelet around the zero frequency varies linearly. Whereas the second-derivative wavelet has non-linear response. This difference may affect the reconstructed 3D profile.

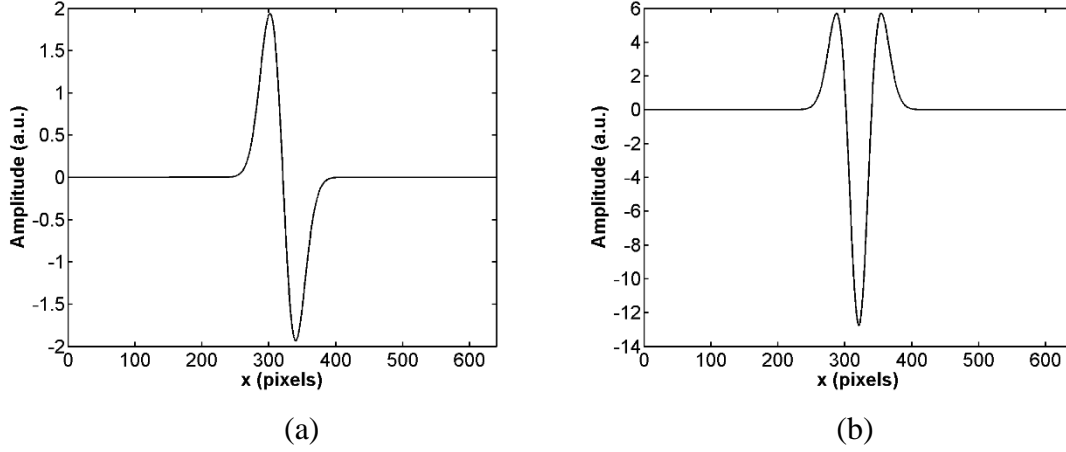


Figure 2.2 (a) First and (b) second derivatives of the Gaussian wavelets, respectively.

After modulating the frequency spectrum of the grating image $g_1(x,y)$ along the horizontal axis f_x by using the dilated wavelet filter $G_1(f_x)H_a^*(f_x,y)$ with the y axis being fixed, one of the fundamental spectra is selected and inversed Fourier transform. The same operation is done for the grating deformed by the screen. As a result, Eqs. (1) and (2) reduce to

$$g'(x, y) = 0.5bo(x, y) \exp[i\phi(x, y)]/c_r' \quad (15)$$

and

$$g''(x, y) = 0.5br(x, y) \exp[i\phi_0(x, y)]/c_r'', \quad (16)$$

respectively. The phase can be extracted from by taking a complex logarithm of the product of Eq. (15) and the conjugate of Eq. (16)

$$\begin{aligned} \log\{g'(x, y)g''^*(x, y)\} = \log[0.25b^2o(x, y)r(x, y)/c_r'c_r''] \\ + i[\phi(x, y) - \phi_0(x, y)] \end{aligned} \quad (17)$$

Finally, the height distribution is calculated according to

$$h(x, y) = \frac{l_0[\phi(x, y) - \phi_0(x, y)]}{[\phi(x, y) - \phi_0(x, y)] - 2\pi f_0 d}, \quad (18)$$

where l_0 and d are the separation distances between the CCD camera and the reference plane and between the camera and the projector.

Chapter 3. Materials and Methods

In order to verify feasibility of our proposed method, an isosceles triangle shown in Fig. 3.1 with dimension of $13\text{ cm} \times 7\text{ cm} \times 4\text{ cm}$ was employed as the test object. The uniform light and the sinusoidal grating pattern were projected from a LCD projector (Toshiba TLP-X2000) with resolution 1024×768 pixels. The four images were recorded by using the CCD camera (Hamamatsu C5948) with resolution 640×480 pixels in $8.3\text{ mm} \times 6.3\text{ mm}$ sensor area and saved into tiff format. The distances l_0 and d were 100 cm and 53 cm , respectively. The grating pitch at the reference plane was 5.35 mm . All computations were done by using Matlab.



Figure 3.1 An isosceles triangular object.

4.1 Experimental Setup of the Frings Projection

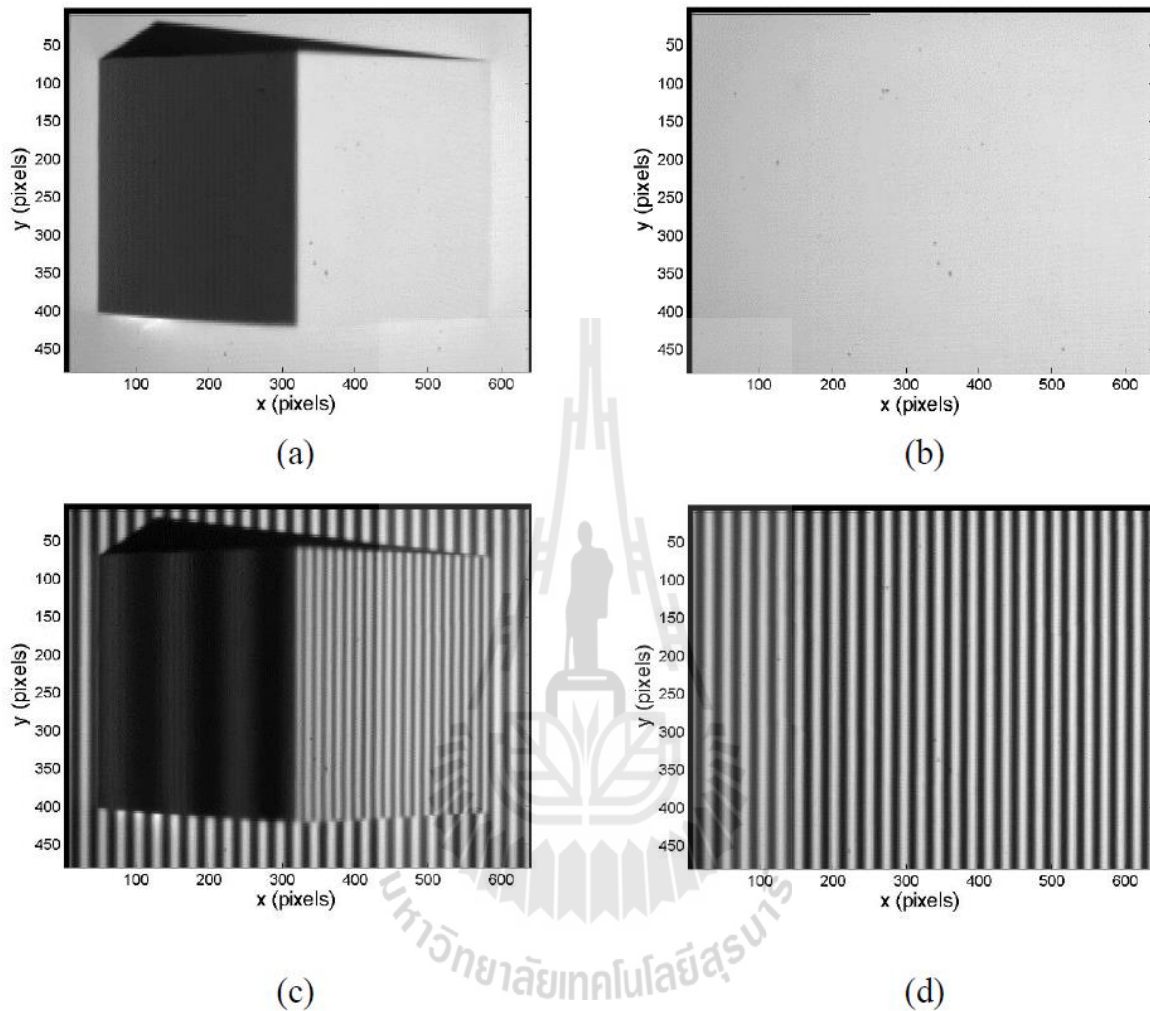


Figure 4.1 Images of (a) the prism object and (b) the reference plane generated by using uniform light. (c) Grating patterns deformed by (a) the object and (d) Grating patterns on the reference plane in (b).

Figures 4.1 (a) and (b) show the images of the object and the reference plane, respectively; their corresponding deformed grating images are shown in Figs. 4.1 (c) and (d). Figures 4.2 (a) and (b) show the image intensities scanned at the row 100th of the grating image deformed by the object and the reference plane, respectively. It is clear that both amplitude and phase of the grating patterns are modulated by the profiles of the object and the reference plane. Due to different reflectivity and height, the two images have different dc

bias levels. The resultant background elimination obtained by computing Eqs. (4) and (5) are shown in Figs. 4.2 (c) and (d). They have zero dc biases.

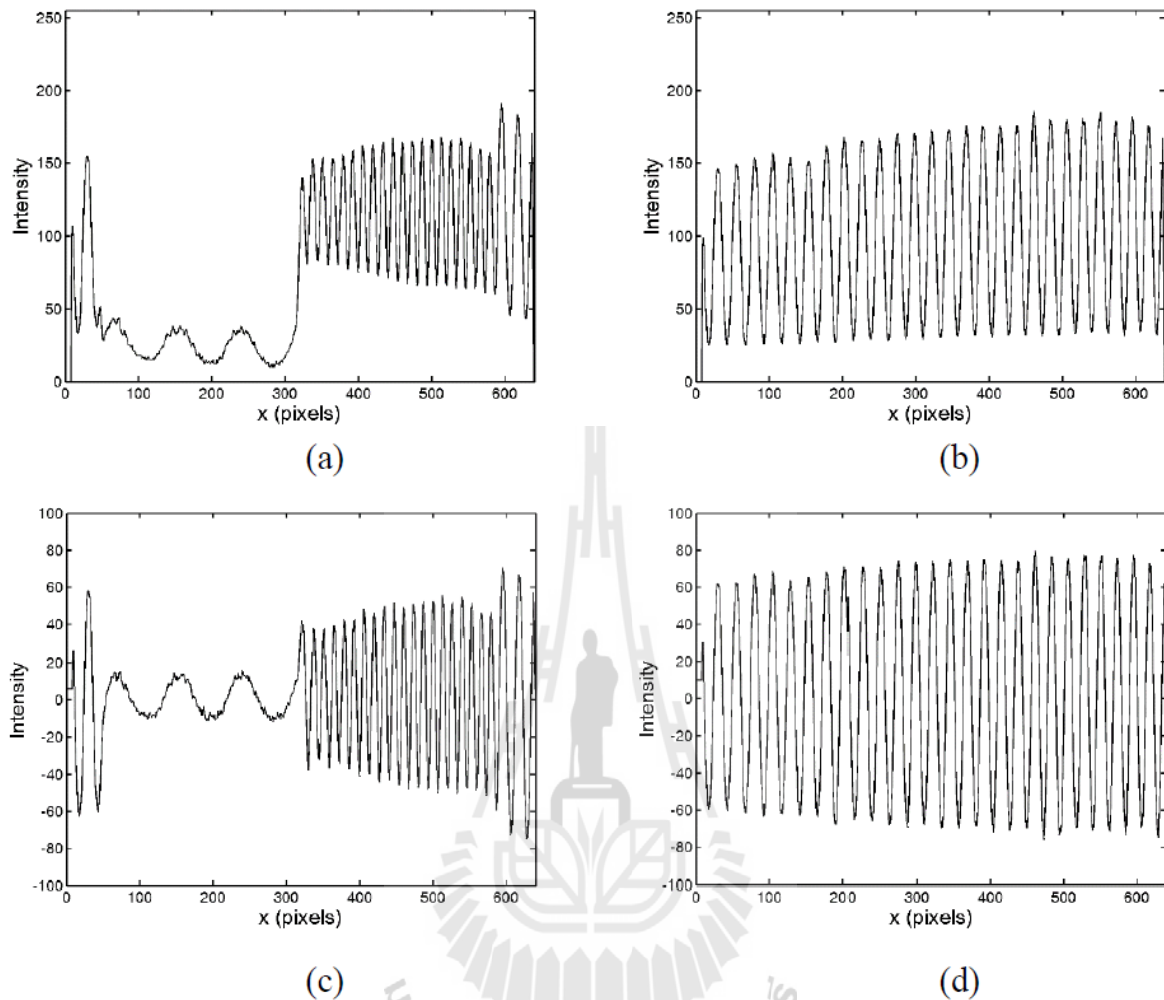


Figure 4.2 Intensities scanned at the row 100th of the grating images deformed by (a) the object and (b) the reference plane. The resultant signals obtained by eliminating the background from (c) Fig. 4.2 (a) and (d) Fig. 4.2 (b).

4.2 3D Height Reconstruction Using DC Subtraction

Figures 4.3 (a) and (b) correspond to the power spectra of the two signals shown in Figs. 4.2 (a) and (c), respectively. In the conventional FTP, besides its high amplitude and broad spectral width, the presence of the zeroth-order spectrum causes problem in localizing the fundamental spectra. The Frequency spectrum of the same grating image obtained by the proposed background elimination is shown in Fig. 4.3 (b). It is obvious from this figure that the fundamental spectra with broad spectral width can be clearly identified.

Figure 4.4 shows the reconstructed height distribution obtained by using the conventional FTP and the proposed method. The band-pass filter used to select the fundamental spectrum had cutoff frequencies of 0.6016 and 8.1211 lp/mm. It is clear that the conventional FTP fails to reconstruct the surface, because the low cutoff frequency of the filter which is closed to zero overlaps with the zero-order spectrum. In contrast, the proposed method does not have difficulty in selecting the fundamental frequency. 8 cm height of the object and the reference plane which has zero height can be correctly reconstructed.

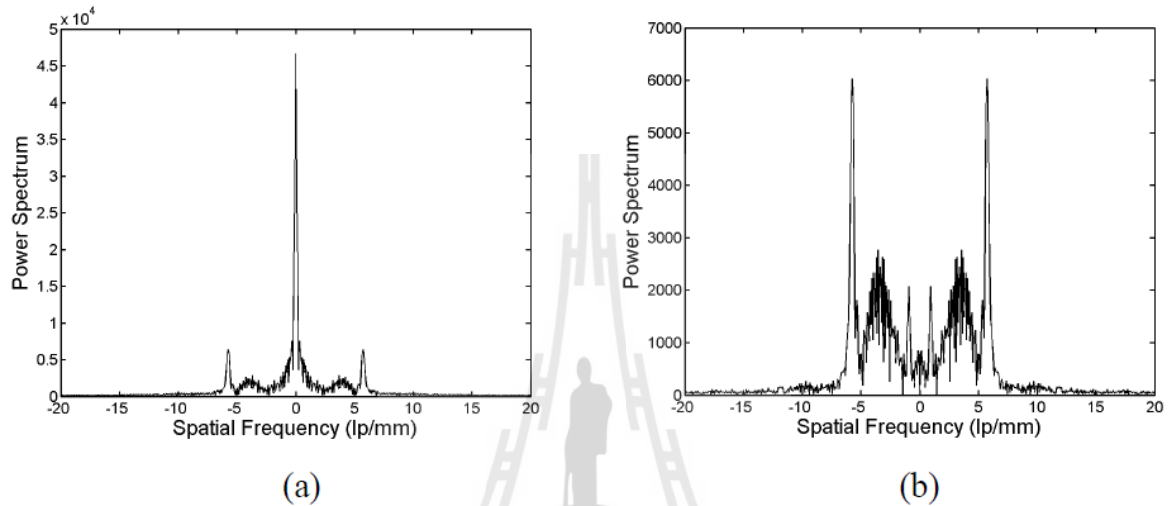


Figure 4.3 Power spectra of the grating pattern deformed by the object obtained by using (a) the conventional FTP and (b) the proposed method.

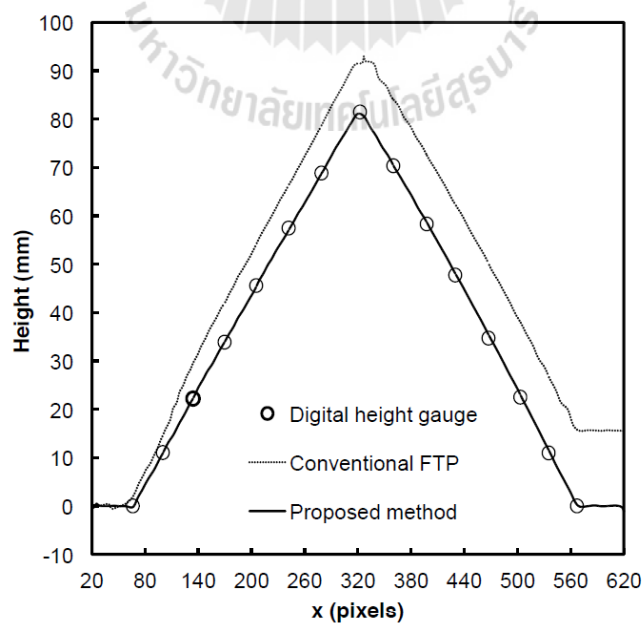


Figure 4.4 Comparison between the height profiles reconstructed by using the conventional FTP, the direct contact and the proposed method.

4.3 3D Height Reconstruction Using the Wavelet transformation

Figure 4.5 shows the reconstructed height distribution obtained by using the conventional FTP and the proposed first derivative of the Gaussian wavelet. It can be observed that the conventional FTP fails to reconstruct the prism profile. Besides its reconstructed surface is not smooth, the base and the peak of the prism do not have correct values. This is because the desired fundamental frequency of the grating deformed by the object is degraded by the zero-order spectrum and the effect of the discontinuity of the rectangular band-pass filter. In contrast, although the prism peak cannot be correctly reconstructed, the use of the Gaussian wavelet gives smoother surface profile and correct height. This may be caused by the linear response of the wavelet filter which removes only the zero frequency.

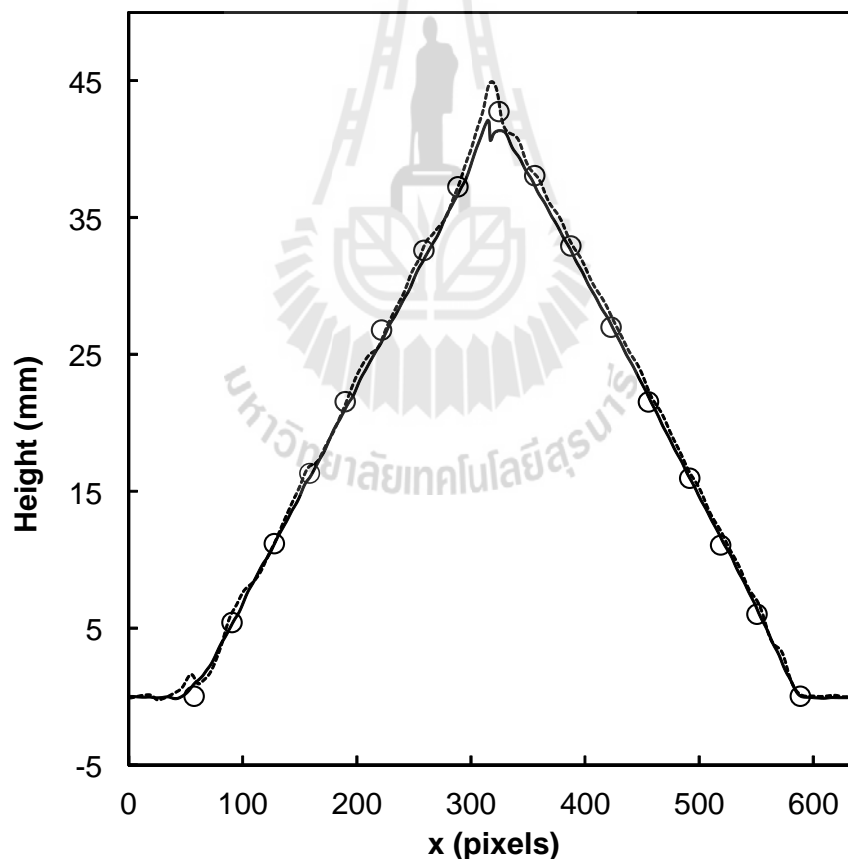


Figure 4.5 Height reconstructions of the prism generated by using the conventional FTP and the first derivative Gaussian wavelet.

The comparison of the reconstructed heights obtained by using the conventional FTP and the second derivative of the Gaussian wavelet is shown in Fig. 4.3. It is apparent that in comparison with Fig. 4.2, the second derivative Gaussian wavelet does not only reconstruct smoothly and accurately the prism surface, but also the peak. The error in measurement of the peak height is 3.22%. This improved result is caused by the nonlinear frequency response of the second order derivative which filters out the low frequency components, instead of only the zero frequency.

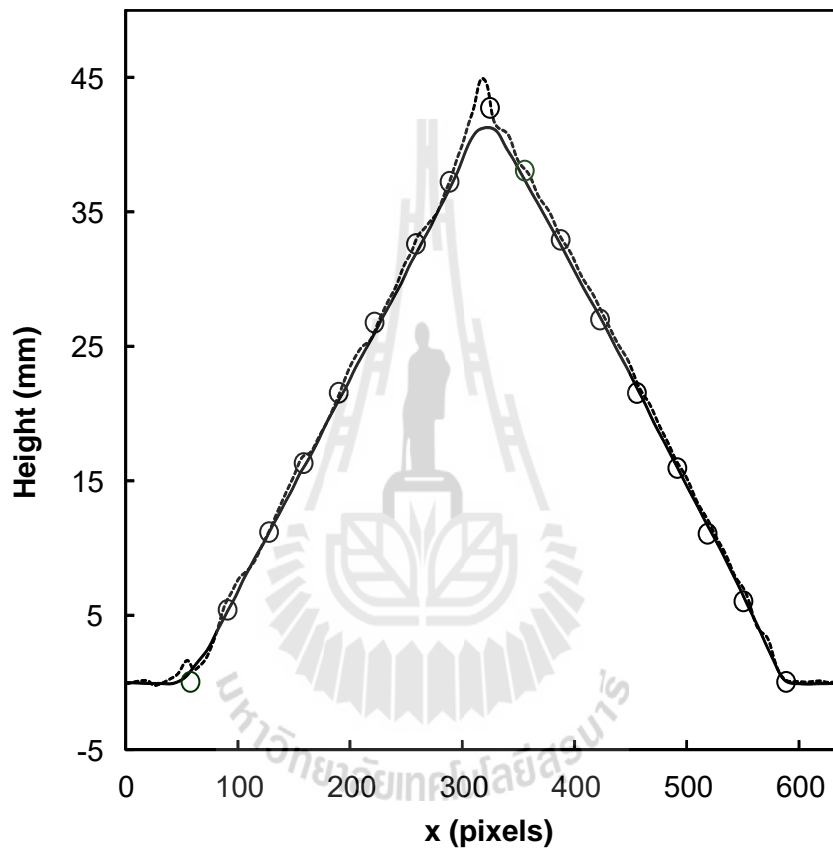


Figure 4.6 Height reconstructions of the prism generated by using the conventional FTP and the second derivative Gaussian wavelet.

Chapter 5. Conclusions

In this research project, we have investigated two techniques for eliminating unwanted background in FTP. In the first technique, by using an object image being measured and a single grating image deformed by this object, the background signal of the deformed grating image can be eliminated by using the object image scaled by a contrast ratio of the two images. In the second technique, the background noise is eliminated by utilizing the wavelet transformation.

In the first project, we have proposed and verified experimentally a new method for the 3D height profile reconstruction by using the FTP with the dc background subtraction method. In order to remove the space-varying dc signal, the proposed method employed images of the object and the reference plane. The experimental verifications show that the proposed method can reconstruct the 3-D object height although the original fundamental spectra are corrupted by the zeroth-order spectrum. The proposed method also has an advantage over the π -phase shifting technique in that less projected grating is used.

In the second project, we have studied the background elimination in the FTP by using the first and the second derivatives of the Gaussian wavelets. The advantage of using the Gaussian wavelets over the conventional rectangular filter of the conventional FTP is that it can simultaneously eliminate the zero order spectrum and localize particular frequency components of signals being analyzed for the height reconstruction. The experimental results show that the 3D height measurements by using the second derivative Gaussian wavelet is more accurate than the first derivative.

Both two proposed methods have advantages over the previous works in that firstly, uses of a white light illumination and a monochrome image sensor results in low-cost system. Moreover, the calibration process of the mean and the contrast values is simpler and independent upon characteristics of the image sensors. In addition, the use of a single grating pattern minimizes simultaneously projection and image acquisition times and phase error caused by abrupt change in amplitude or timing of light projector's synchronization signals known as jitters.

Research Outcome

- 1) We have develop a laboratory prototype of the FTP for non-destructive and non-contact 3D profilometry based on grating pattern projection.
- 2) We have developed two signal processing techniques to eliminate background noise and improve the performance of the FTP technique.
- 3) Two master student have been involved in this project
 - Mr.JAROON WONGJARERN, Studet ID: M5410132, a M.S. student under the program of Laser Technology and Photonics, Institute of Science, Suranaree University of Technology
 - Mr.THAWEESAK CHAIYAKHUN, Student ID: M5710126, a M.S. student under the program of Applied Physics, Institute of Science, Suranaree University of Technology
- 4) Presentation at the International Conference on Experimental Mechanics 2013 and the Twelfth Asian Conference on Experimental Mechanics, at Bangkok, Thailand, during November 25-27, 2013.
 - J. Wongjarern, J. Widjaja, W. Sangpech, N. Thongdee, P. Santisoonthornwat, O. Traisak, P. Chuamchaitrakool, P. Meemon “Fourier transform profilometry by using digital dc subtraction”, *Proc. SPIE* **9234**, pp 923412 (2013).
- 5) One publication in the -International Journal for Light and Electron Optics (Optik)
 - Jaroon Wongjarern, Joewono Widjaja, Porntip Chuamchaitrakool, Panomsak Meemon, “Non-phase-shifting Fourier transform profilometry using single grating pattern and object image” *Optik* 127(19), 7565-7571 (2016).

References

1. M. Takeda, H. Ina and S. Kobayashi, "Fourier-transform method of fringe-pattern analysis for computer-based topography and interferometry," *J. Opt. Soc. Am.* 72, 156 - 160 (1982).
2. M. Takeda and K. Mutoh, "Fourier transform profilometry for the automatic measurement of 3-D object shapes," *Appl. Opt.* 22(24), 3977 - 3982 (1983).
3. D.R. Burton, A.J. Goodall, J.T. Atkinson and M.J. Lalor, "The use of carrier frequency shifting for the elimination of phase discontinuities in Fourier transform profilometry," *Opt. Lasers Eng.* 23, 245 - 257 (1995).
4. H.M Yue, X.Y. Su and Y.Z. Liu, "Fourier transform profilometry based on composite structured light pattern," *Opt. Laser Tech.* 39, 1170 - 1175 (2007).
5. E. Hu and F. Haifeng, "Surface profile inspection of a moving object by using dual-frequency Fourier transform profilometry," *Optik* 122, 1245 - 1248 (2011).
6. Y. Fu, J. Wu and G. Jiang, "Fourier transform profilometry based on defocusing," *Opt. Laser Tech.* 44, 727 - 733 (2012).
7. M. Leonardi, M. Flezar, A. Urbanc and J. Lenarcic, "Application of Fourier transform profilometry in pulmonary function testing," *J. Compt. Inf. Tech.* 2, 223 - 231 (1994).
8. M. Leonardi, M. Cucek-Plenicar and J. Lenarcic, "Application of Fourier Transform Profilometry for Measurements of Human Back," in *Studies in Health Technology and Informatics 37*, Eds. J.A. Sevastik and K.M. Diab, IOS Press, 319 - 322 (1997).
9. F. Lilley, M. J. Lalor and D. R. Burton, "Robust fringe analysis system for human body shape measurement," *Opt. Eng.* 39, 187 - 195 (2000).
10. L. Chen and C. Huang, "Miniaturized 3D surface profilometer using digital fringe projection," *Meas. Sci. Tech.* 16, 1061 - 1068 (2005).
11. A. Hanafi, T. Gharbi and J. Cornu, "In vivo measurement of lower back deformations with Fourier-transform profilometry," *Appl. Opt.* 44, 2266 - 2273 (2005).
12. L.D. Stefano and F. Boland, "Solder-paste inspection by structured light methods based on phase measurement," *Proc. SPIE 2899, Automated Optical Inspection for Industry*, 702 (1996).
13. C. Quan, C.J. Tay, X.Y. Heb, X Kang and H.M. Shang, "Microscopic surface contouring by fringe projection method," *Opt. Lasers Eng.* 34, 547 - 552 (2002).
14. H. Yen, D. Tsai and J. Yang, "Full-field 3-D measurement of solder pastes using LCD-based phase shifting techniques," *IEEE Trans. Elect. Pack. Manu.* 29, 50 - 57 (2006).

15. T. Hui and G. K. Pang, "Solder paste inspection using region-based defect detection," *Int. J. Adv. Manu. Tech.* 42, 725 - 734 (2009).
16. D. Hong, H. Lee, M. Y. Kim, H. Cho and J. Moon, "Sensor fusion of phase measuring profilometry and stereo vision for three-dimensional inspection of electronic components assembled on printed circuit boards," *Appl. Opt.* 48, 4158 - 169 (2009).
17. S. Tan, D. Song and L. Zeng, "Tracking fringe method for measuring the shape and position of a swimming fish," *Opt. Commun.* 173, 123 - 128 (2000).
18. P. Cheng, J. Hu, G. Zhang, L. Hou, B. Xu and X. Wu, "Deformation measurements of dragonfly's wings in free flight by using Windowed Fourier Transform," *Opt. Laser Eng.* 46, 157 - 161 (2008).
19. G.H. Wua, L.J Zeng and L.H. Ji, "Measuring the wing kinematics of a moth (*Helicoverpa Armigera*) by a two-dimensional fringe projection method," *J. Bionic Eng.* 5, 138 - 142 (2008).
20. G. S. Spagnolo, D. Ambrosini and D. Paoletti, "Low-cost optoelectronic system for three-dimensional artwork texture measurement," *IEEE Trans. Image Proc.* 1, 390 - 396 (2004).
21. G. Sansoni and F. Docchio, "3-D optical measurements in the field of cultural heritage: The case of the Vittoria Alata of Brescia," *IEEE Trans. Inst. Meas.* 5, 359 - 368 (2005).
22. P.J. Cobelli, A. Maurel, V. Pagneux and P. Petitjeans, "Global measurement of water waves by Fourier transform profilometry," *Exp. Fluids* 46, 1037 - 1047 (2009).
23. A. Martinez, J.A. Raya, R.R. Cordero, D. Balieiroc and F. Labbe, "Leaf cuticle topography retrieved by using fringe projection," *Opt. Lasers Eng.* 50, 231 - 235 (2012).
24. B.C. Redman, S.J. Novotny, T. Grow, V. Rudd, N. Woody, M. Hinckley, P. McCumber, N. Rogers, M. Hoening, K. Kubala, S. Shald, R. Uberna, T. D'Alberto, T. Hoft, R. Sibell, and F.W. Wheeler, "Stand-off Biometric Identification using Fourier Transform Profilometry for 2D+3D Face Imaging," *CLEO 2011: Applications and Technology (CLEO: A and T) paper: ATuF4.*
25. M.A. Gdeistat, D.R. Burton, M.J. Lalor, "Eliminating the zero spectrum in Fourier transform profilometry using a two-dimensional continuous wavelet transform," *Opt. Commun.* 266, 482 - 489 (2006).
26. A Dursun, S Özder, FN Ecevit, "Continuous wavelet transform analysis of projected fringe patterns," *Meas. Sci. Technol.* 15, 1768- (2004).
27. S. Mallat and, W.L. Hwang, "Singularity detection and processing with wavelets," *IEEE Trans. Inf. Theory* 38, 617 - 643 (1992).

ประวัตินักวิจัย

ศาสตราจารย์ ดร. โจโวโน วิดจาญา (Joewono Widjaja) เป็นอาจารย์ประจำสาขาวิชาฟิสิกส์ สำนักวิชาวิทยาศาสตร์ มหาวิทยาลัยเทคโนโลยีสุรนารี จบการศึกษาระดับปริญญาตรีวิศวกรรมศาสตรบัณฑิต (สาขาวิศวกรรมอิเล็กทรอนิกส์) จาก Satya Wacana Christian University, Indonesia (1986) และสำเร็จการศึกษาระดับปริญญาโท (Master of Engineering) และปริญญาเอก (Doctor of Engineering) ในสาขาวิชาวิศวกรรมอิเล็กทรอนิกส์ จาก Hokkaido University, Japan ในปี พ.ศ. 2534 และ 2537 ตามลำดับ สาขางานวิจัยที่มีความชำนาญพิเศษคือ การประมวลผลสัญญาณเชิงแสง ดิจิตอลโฮโลแกรม และมาตรวิทยาเชิงแสง

สถานที่ติดต่อ: อาคารวิชาการ 2 ชั้น 5 ห้อง C2-542 สาขาวิชาเทคโนโลยีเลเซอร์และโฟโตนิกส์ สำนักวิชาวิทยาศาสตร์ มหาวิทยาลัยเทคโนโลยีสุรนารี เลขที่ 111 ถนนมหาวิทยาลัย ต. สุรนารี อ. เมือง จ. นครราชสีมา 30000 โทร. 044 224 194 หรือ Email: widjaja@sut.ac.th

ผศ.ดร. พนมศักดิ์ มีมนต์ (Panomsak Meemon) เป็นอาจารย์สาขาวิชาฟิสิกส์ สำนักวิชาวิทยาศาสตร์ มหาวิทยาลัยเทคโนโลยีสุรนารี จบการศึกษาระดับปริญญาตรี วิศวกรรมศาสตรบัณฑิต (สาขาวิศวกรรมไฟฟ้า) จากคณะวิศวกรรมศาสตร์ มหาวิทยาลัยเชียงใหม่ ในปี พ.ศ. 2543 จากนั้นในปี พ.ศ. 2547 ได้รับทุนรัฐบาลซึ่งจัดสรรโดยกระทรวงวิทยาศาสตร์และเทคโนโลยีแห่งชาติ เพื่อศึกษาต่อในระดับปริญญาโท (Master of Science) และปริญญาเอก (Ph.D.) ในสาขาวิชา Optics จาก College of Optics and Photonics, University of Central Florida, USA ปีที่สำเร็จการศึกษา พ.ศ. 2553 หลังจบการศึกษาระดับปริญญาเอกแล้วได้ทำงานเป็นนักวิจัยที่ Optical Diagnostics and Applications Laboratory, Institute of Optics, University of Rochester, USA เป็นเวลา 1 ปี ก่อนมารับตำแหน่งเป็นอาจารย์ ในสาขาวิชาเทคโนโลยีเลเซอร์และโฟโตนิกส์ สำนักวิชาวิทยาศาสตร์ ในปี พ.ศ. 2554 จนถึงปัจจุบัน สาขางานวิจัยที่มีความชำนาญพิเศษคือ การออกแบบระบบเชิงแสง โดยเน้นการพัฒนากระบวนการถ่ายภาพสามมิติด้วยแสงอินฟราเรดและการประยุกต์ในเชิงชีวการแพทย์และชีววิทยา

สถานที่ติดต่อ: อาคารวิชาการ 2 ชั้น 5 ห้อง C2-537 สาขาวิชาเทคโนโลยีเลเซอร์และโฟโตนิกส์ สำนักวิชาวิทยาศาสตร์ มหาวิทยาลัยเทคโนโลยีสุรนารี เลขที่ 111 ถนนมหาวิทยาลัย ต. สุรนารี อ. เมือง จ. นครราชสีมา 30000 โทร. 044 224 544 หรือ Email: panomsak@sut.ac.th